*Protein Science* (2000), *9*:916–926. Cambridge University Press. Printed in the USA.


# Comparative model building of interleukin-7 using interleukin-4 as a template: A structural hypothesis that displays atypical surface chemistry in helix D important for receptor activation

LARRY COSENZA,[1,2] ANDREW ROSENBACH,[3] JAMES V. WHITE,[4] JOHN R. MURPHY,[1] AND TEMPLE SMITH[3]

[1]Section of Biomolecular Medicine, Evans Department of Clinical Research and Department of Medicine, Boston University School of Medicine, Boston, Massachusetts 02118-2393
[2]Departments of Pharmacology and Experimental Therapeutics and Medicine, Boston University School of Medicine, Boston, Massachusetts 02118-2393
[3]BioMolecular Engineering Research Center, College of Engineering, Boston University, Boston, Massachusetts 02215
[4]JVWhite.Com, 5 Kelly Road, Cambridge, Massachusetts 02139

(RECEIVED November 10, 1999; FINAL REVISION March 20, 2000; ACCEPTED March 23, 2000)

**Abstract**

Using a combination of theoretical sequence structure recognition predictions and experimental disulfide bond assignments, a three-dimensional (3D) model of human interleukin-7 (hIL-7) was constructed that predicts atypical surface chemistry in helix D that is important for receptor activation. A 3D model of hIL-7 was built using the X-ray crystal structure of interleukin-4 (IL-4) as a template (Walter MR et al., 1992, *J Mol Biol. 224*:1075–1085; Walter MR et al., 1992, *J Biol Chem 267*:20371–20376). Core secondary structures were constructed from sequences of hIL-7 predicted to form helices. The model was constructed by superimposing IL-7 helices onto the IL-4 template and connecting them together in an up–up down–down topology. The model was finished by incorporating the disulfide bond assignments (Cys3, Cys142), (Cys35, Cys130), and (Cys48, Cys93), which were determined by MALDI mass spectroscopy and site-directed mutagenesis (Cosenza L, Sweeney E, Murphy JR, 1997, *J Biol Chem 272*:32995–33000). Quality analysis of the hIL-7 model identified poor structural features in the carboxyl terminus that, when further studied using hydrophobic moment analysis, detected an atypical structural property in helix D, which contains Cys130 and Cys142. This analysis demonstrated that helix D had a hydrophobic surface exposed to bulk solvent that accounted for the poor quality of the model, but was suggestive of a region in IL-7 that maybe important for protein interactions. Alanine (Ala) substitution scanning mutagenesis was performed to test if the predicted atypical surface chemistry of helix D in the hIL-7 model is important for receptor activation. This analysis resulted in the construction, purification, and characterization of four hIL-7 variants, hIL-7(K121A), hIL-7(L136A), hIL-7(K140A), and hIL-7(W143A), that displayed reduced or abrogated ability to stimulate a murine IL-7 dependent pre-B cell proliferation. The mutant hIL-7(W143A), which is biologically inactive and displaces [$^{125}$I]-hIL-7, is the first reported IL-7R system antagonist.

**Keywords:** alanine scanning; interleukin-7; homology modeling; protein fold recognition

The cytokine structural superfamily is composed of a diverse group of growth factors that have markedly dissimilar amino acid sequences. The cytokine superfamily has been subdivided into groups, each of which exemplifies typical protein folds such as an alpha-parallel bundle (Sprang & Bazan, 1993). In general, mutational studies have defined three sites that can be involved in receptor binding in the alpha-parallel bundle family of cytokines. Amino acid residues located in these sites appear to cluster on helices A and D and the long loops A–B and C–D (Mott & Campbell, 1995). In addition, amino acid sequence comparisons of their respective cell surface receptors display shared related sequences in their extracellular domains (Bazan, 1990b). Given these observations, it is reasonable to postulate that there may be an overall similarity in the molecular mechanism of ligand receptor binding and subsequent target cell activation in the cytokine superfamily (Wlodawer et al., 1993).

Reprint requests to: Temple Smith, Boston University, BioMolecular Engineering Research Center, 36 Cummington Street, Boston, Massachusetts 02215; e-mail: tsmith@darwin.bu.edu.

*Abbreviations:* CD, circular dichroism; DSM, discrete state-space model; EDTA, ethylenediaminetetraacetic acid; GM-CSF, granulocyte-macrophage colony stimulating factor; GH, growth hormone; HPLC, high performance liquid chromatography; IL-4, interleukin-4; IL-7, interleukin-7; IPTG, isopropyl-$\beta$-D-thiogalactopyranoside; MALDI, matrix-assisted laser desorption ionization; PSA, protein sequence assignment; R, receptor.

Interleukin-7 is a cytokine that stimulates pre-B-cell (Goodwin et al., 1989; Namen et al., 1988) and mature T-cell proliferation (Chazen et al., 1989; Welch et al., 1989; Londei et al., 1990). Interestingly, IL-7 can induce lymphokine-activated killer (LAK) cells and cytolytic T-cells (Alderson et al., 1991). The importance of these observations has been underscored in transgenic mice where the expression of IL-7 or IL-7 receptor has been genetically enhanced or eliminated (Mertsching et al., 1997; Maeurer & Lotze, 1998; Watanabe et al., 1998). These transgenic mice display gross morphological differences in thymus and spleen with B-cell development restricted to pre-B ($B220^+$, $IgM^-$) and earlier development (Mertsching et al., 1997; Maki et al., 1998). This is in contrast to interleukin-2 (IL-2) and IL-4 transgenic mice in which elimination of expression of either of these cytokines has been compensated by redundancies in the immune system (Di Santo et al., 1995). Thus, IL-7 is an important regulating factor for the normal development of both B- and T-cells and may have therapeutic applications in cancer immune therapy (Murphy et al., 1993) and treatment of immune deficiency diseases. Although IL-7 has important therapeutic potential, little is known of its tertiary structure and structure function relationships.

In this paper we describe an atomic scale model of hIL-7 that was constructed by comparative model building, using the X-ray crystal structure of human IL-4 as a template (Bajorath et al., 1993), followed by alanine (Ala)-substitution scanning mutagenesis analysis that defined structure–function relationships important for receptor activation. Initially, a sequence structure recognition analysis designed by Stultz et al. (1997), directly linked the amino acid sequence of hIL-7 with a probabilistic model representing an alpha-parallel bundle tertiary protein fold. Circular dichroism (CD) analysis supports the prediction that hIL-7 is a predominant alpha-helical structure. This analysis resulted in assigning secondary structural elements to the hIL-7 amino acid sequence. The X-ray crystal structures of two human alpha-parallel bundle cytokine superfamily proteins, IL-4 (Walter et al., 1992b) and granulocyte macrophage colony-stimulating factor, GM-CSF (Walter et al., 1992a), were used as three-dimensional (3D) templates to build IL-7 models. The IL-4–derived model was further developed based upon overall folding and functional class membership considerations and the number of disulfide bonds in the structure.

Incorporating disulfide bond assignments generated from mass spectroscopy and mutational analysis of recombinant hIL-7 further refined the IL-4–derived IL-7 model. Incorporation of disulfide bond assignments into the hIL-7 model forced a reorientation of helix D, thus exposing a hydrophobic surface to solvent. The solvent exposed hydrophobic surface on helix D in the hIL-7 model resulted in poor structural evaluations compared to a previously reported model of hIL-7 (Kroemer et al., 1996). The biological importance of this observation was tested by site-directed Ala substitution scanning mutagenesis and this structure–function analysis defined an IL-7 receptor binding surface. Importantly, this analysis also resulted in the isolation of hIL-7(W143A), a potential IL-7R antagonist.

## Results

### *IL-7 protein fold recognition analysis*

The hIL-7 amino acid sequence was analyzed to determine its probable 3D folding class. The analysis algorithm (Stultz et al., 1993, 1997; White et al., 1994; Yu et al., 1998; PSA e-mail server) uses a library of probabilistic Discrete State-space Models (DSMs) for more than 20 distinguishable protein folding classes. The algorithm assigned each DSM in the library a probability of having generated the hIL-7 amino acid sequence. The highest probability (0.91) was assigned to the DSM for the alpha-bundle folding class, which consists of proteins composed of four helices of roughly equal length connected by loops of different lengths. This analysis suggests that hIL-7 is primarily helical and adopts a cytokine-like fold that has been predicted previously (Parry, 1991). Circular dichroism (CD) analysis suggests that hIL-7 secondary structure is 35% alpha-helical, 31% random coil, 23% beta sheet, and 11% beta turn, which supports the prediction that hIL-7 is primarily an alpha-helical structure (data not shown).

### *Secondary structure predictions based upon an alpha-bundle DSM assignment*

The secondary structural state of each residue in the hIL-7 sequence was estimated using the alpha-bundle DSM and a probabilistic smoothing algorithm (Stultz et al., 1993). The algorithm assigns the probability that each residue is in a helix-exposed, a helix-buried, or a loop state. These probabilities for hIL-7 are displayed as a contour probability map in Figure 1A. There is high

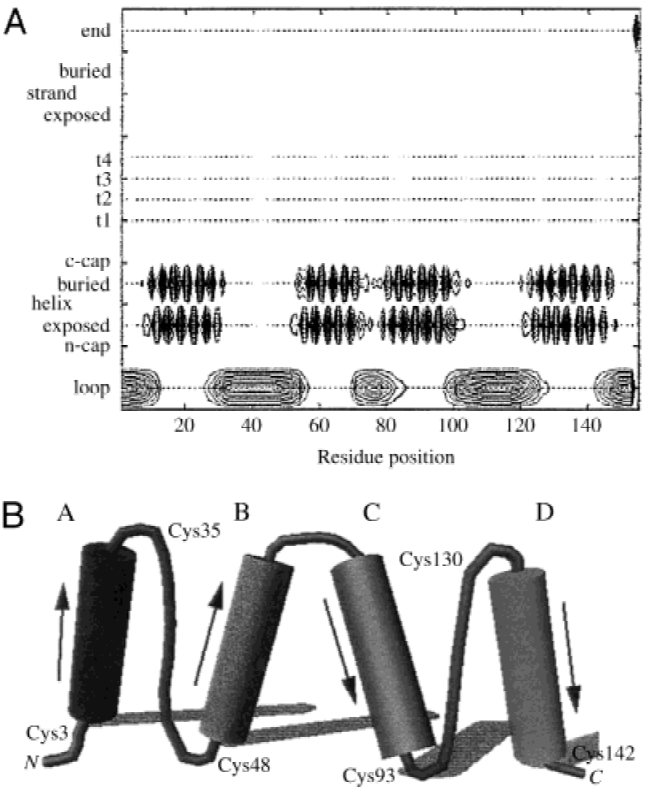


**Fig. 1.** Secondary structure probability assignments for the human IL-7 amino acid sequence. **A:** Contour plot of secondary-structure probabilities with contour lines of constant probability in increments of 0.1. Each row corresponds to a different secondary structural state, and each column corresponds to a different sequence residue position. Areas surrounded by multiple contour lines are regions of high probability. **B:** A graphical representation of alpha-helix and loop placement in IL-7 displaying the conserved cytokine up–up down–down connectivity and the relative placement of cysteine residues.

probability for four alpha-helices, connected with two long and one short loop. The two long loops occur between proposed helices A,B and C,D, which allows the secondary structural topology to assume an up–up down–down connectivity previously seen in the crystal structure of other cytokines and graphically displayed in Figure 1B. Interestingly, a comparison of the secondary structural prediction made by Parry (1991), using his heptad algorithm also recognizes this topology where the methods of Garnier et al. (1978) and Chou and Fasman (1978) did not.

*Construction of an IL-7 structural hypothesis*

Three-dimensional structural models of hIL-7 were constructed using the X-ray crystal structures of IL-4 (Protein Data Bank (PDB) ID: 2INT; Walter et al., 1992a) and GM-CSF (PDB ID: 1CSG; Walter et al., 1992b) as templates, which have an alpha-bundle protein fold. Both the IL-4 and GM-CSF structures represented suitable alpha-parallel bundle fold templates, displayed up–up down–down topology, and are similar in size to IL-7. The IL-4–derived model was further developed based upon overall folding and functional class membership considerations, and the number of disulfide bonds that could be formed in the structure. Briefly, the model of hIL-7 was built by constructing regular alpha-helices from amino acid sequences predicted to form helices from the structure sequence recognition analysis and then superimposed on the secondary structural elements in the IL-4 template. Due to the differences between the lengths of the first helix in the model and the template, helix A of IL-7 was constructed in two parts prior to being superimposed upon the IL-4. IL-7 bioactivity is dependent on disulfide bond formation (Goodwin et al., 1989); therefore, placement of core helices in the first generation models was restricted to ensure that the alpha-carbons of cysteine residues potentially involved in disulfide bond formation were within 4 to 7.5 Å (Fasman, 1989). The remaining hIL-7 amino acid sequences were then modeled in as loops or turns using a bond scaling and relaxing algorithm (Zheng et al., 1992). Disulfide bond assignments in human IL-7 were experimentally determined by MALDI mass spectroscopy and site-directed mutational analyses (Cosenza et al., 1997). These experimental results, which differed from the previously reported disulfide bonds in hIL-7 (Srinivasan et al., 1993), were used as 3D spatial constraints for the final placement and orientation of the core helices in the hIL-7 model. After the disulfide bonds were constructed in the model, the whole structure was energetically minimized to reduce steric clashes and torsional strain. The atomic coordinates of the resultant structure have been deposited in the Protein Data Bank (Bernstein et al., 1977) at Brookhaven National Laboratory, with PDB identification code 1il7. A cartoon of the model is displayed in Figure 2. The hIL-7 protein model contains four helices, starting with the helix closest to the amino terminus, A (4–29), B (45–68), C (75–101), and D (121–147). The helices are oriented in an up–up down–down configuration and compose 60% of the structure. The three disulfide bond assignments are composed of cysteine residue pairs (Cys3, Cys142), (Cys35, Cys130), and (Cys48, Cys93).

*Comparison of the hIL-7 model produced in this work with the IL-4 X-ray crystal structure and a previously reported hIL-7 model*

An amino acid sequence and a secondary structure comparison between the hIL-7 model constructed in this work and the structures for IL-4 and a previously reported model of hIL-7 (Kroemer et al., 1996) are displayed in Figures 3A and 3B. There is a 21.4% amino acid sequence similarity between hIL-7 and hIL-4, and there is no apparent conservation of disulfide bonds between the two proteins (Fig. 3A). There is, however, a disulfide bond in both the IL-4 and IL-7 proteins, (Cys3, Cys127) and (Cys3, Cys142), respectively, which hold the amino and carboxyl termini in close proximity. Comparison of the placement of helices and disulfide bond assignment between the IL-7 models is shown in Figure 3B. Both models maintain four helices with long loops between helix pairs (A, B) and (C, D), which preserves the up–up down–down topology seen in the alpha-helical cytokines. Kroemer et al. (1996) inserts an additional small helix into the long loop between helices A and B. The major difference between the IL-7 models is the disulfide bond assignments. The disulfide bond assignments in the IL-7 model presented in this paper tether the amino and carboxyl terminals of the protein together while the Cys linkages in the model by Kroemer et al. (1996) pin the terminals back on themselves.

A 3D comparison of the structures for both IL-7 models and the IL-4 structure was performed using an automated Multiple Alignment of Protein Structures (MAPS) (Lu, 1996, 1998) tool accessible via the Internet. This program represents secondary structures using a line generated from two points located at the ends of each element. An algorithm then systematically searches all possible

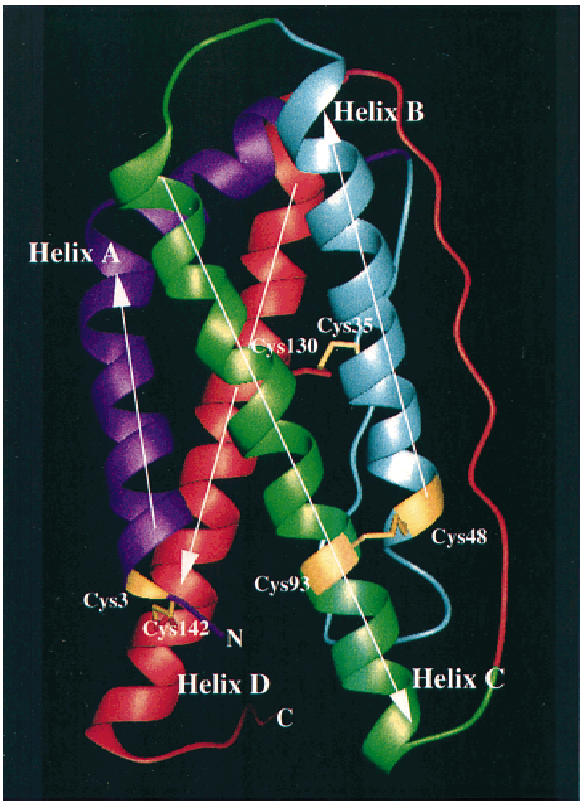


**Fig. 2.** Three-dimensional ribbon structure model of IL-7. Helices are labeled A–D, starting with the N-terminal. The amino and carboxyl termini are labeled N and C, respectively. Helix A is purple, helix B is blue, helix C is green, and helix D is orange. The conserved up–up down–down connectivity of helices are represented by white arrows indicating the amino to carboxyl direction. Disulfide bonds are yellow and labeled (Cys3, Cys142), (Cys48, Cys93), and (Cys35, Cys130).

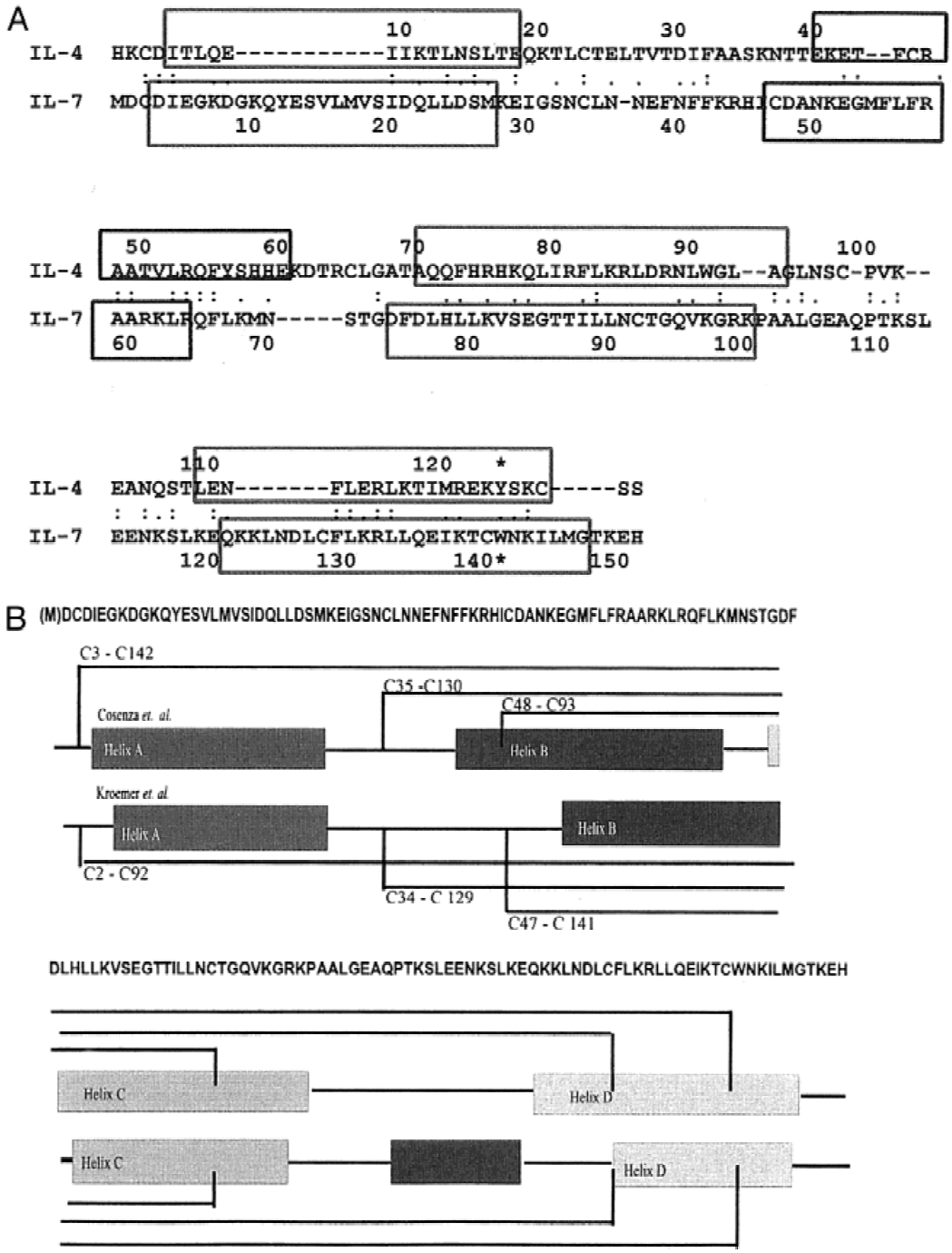


**Fig. 3.** Amino acid sequence and secondary structure comparison between IL-4 and the IL-7 models. **A:** Amino acid sequence alignment between human IL-4 and IL-7. The boxes represent helices found in the IL-4 X-ray crystal structure and predicted by the IL-7 model. **B:** Comparison between the secondary structure placement and disulfide bond assignments between the human IL-7 models of Cosenza et al. (1997) and Kroemer et al. (1996). Amino acid sequence for recombinant human IL-7 is shown, with methionine in parentheses. Helices are represented as boxed regions and disulfide bonds by cross-connecting lines.

superpositions of the elements between two structures. The C$\alpha$ coordinates from residues in matched elements are used to calculate root-mean-square (RMS) and mean differences in angstroms (Å), and the angles between superimposed matched line elements are recorded. A similarity between structures is claimed if a number of secondary structural elements can be matched. A comparison score, topological diversity (TD), is computed, which uses the rate of matching secondary structural elements and the RMS difference the C$\alpha$ atoms in matched amino acid residues. As the number of matched secondary structural elements increases the TD score decreases; hence, low scores indicate structural similarity. A TD score of 0 means the structures are identical.

A comparison between the IL-4 structure and IL-7 models using MAPS suggests that all elements are topologically similar. Comparison between the IL-7 models and the IL-4 structure suggests that the IL-7 models have larger topological differences when compared to each other than when compared to IL-4. Comparison of the IL-4 (129 aa) structure and our IL-7 model (153 aa) results in matching 58 residues that are in topologically equivalent positions, with an average RMS difference between the matched C$\alpha$ atoms of 1.35 Å, a mean distance difference of 1.21 Å, and a TD score of 11.5. MAPS comparison between the IL-4 structure and the IL-7 model (152 aa) of Kroemer et al. matched 37 residues that are in topologically equivalent positions, an average RMS difference between the matched C$\alpha$ atoms of 1.87 Å, a mean distance difference of 1.71 Å, and a TD score of 10.2. A comparison between the IL-7 model constructed in this project and the Kroemer et al. structure resulted in matching 48 residues that are topologically equivalent positions, an average RMS difference between matched C$\alpha$ atoms of 2.08 Å, a mean distance difference of 1.95 Å, and a TD score of 13.9. All of the computations are presented in Table 1, and a graphical representation of the superimposed ribbon structures for the IL-7 models is shown in Figure 4.

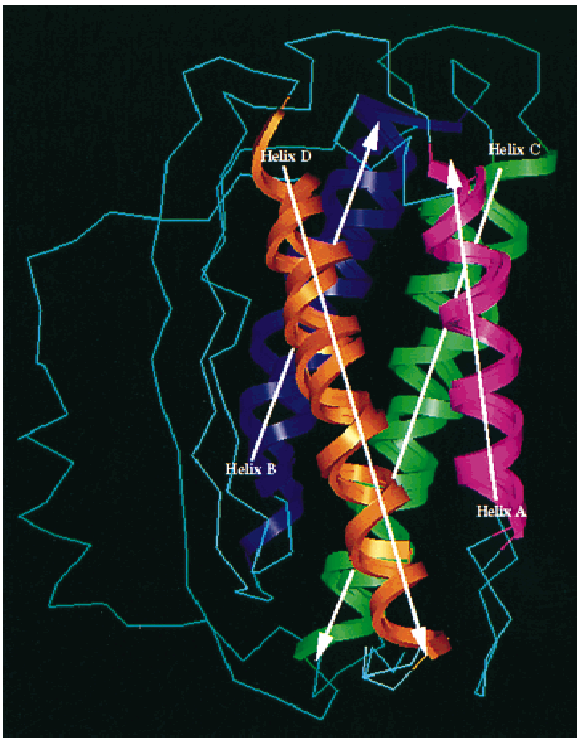


**Fig. 4.** Graphical representation of the superimposed IL-7 models of Cosenza et al. (1997) and Kroemer et al. (1996). The coordinates from the IL-7 model generated in this work and that from Kroemer et al. (1996) are superimposed maximizing the helical backbone overlap. Helices A–D are labeled and colored as in Figure 2.

### *3D–1D profile evaluation of the IL-4 structure and IL-7 models*

The quality of the IL-4 template and IL-7 models was evaluated using Verify3D (Luthy et al., 1992). This analysis measures the compatibility, a profile score (S), between a structure and its sequence using the statistical preferences for each amino acid residue to occur in a particular secondary structure. The results are displayed in Figure 5; the average 3D–1D profile score for a 21-residue sliding window is plotted vs. the residue number. A profile score for a particular structure is the sum, over all residue positions, of the statistical structure preferences for the amino acid sequence of the protein. The profile score depends on the size and validity of the structure and increases with length. Analysis of the IL-4 structure demonstrates good overall structure with a profile score of 59.89. The computed profile score of the Kromer et al. IL-7 model is 44.23 and that of the IL-7 model generated in this work is 13.55, the lowest quality of the structures compared. A major difference in the profile score is shown in the carboxyl terminal of the IL-7 model generated in this work compared to the IL-4 template and the Kroemer et al. model. We believe that this is a result of the disulfide bond assignment (Cys3, Cys142) in hIL-7 forcing a reorientation of helix D.

### *Hydrophobic moment analysis of the IL-7 model*

The poor quality of our IL-7 model was investigated further using a hydrophobic moment analysis of the secondary structural elements. This analysis calculated a hydrophobic moment for helix D in the IL-7 model generated in this work that was oriented toward bulk solvent and may indicate a region on the surface of the structure important for receptor binding. The structural moments of the amino acid residues that form the helices in the IL-7 protein model were calculated, vectorially summed, and then graphically displayed (Eisenberg et al., 1982) (Fig. 6A,B). The moments for the first three predicted helices in the IL-7 model are oriented toward the center of the structure; the calculated hydrophobic moment of helix D is orientated toward bulk solvent.

**Table 1.** *Summary of results from the comparison of IL-4 and IL-7 models*

| Structure | Size (residues) | IL-4 aa similarity | IL-7[a] (Cosenza et al., 1977) | IL-7[a] (Kroemer et al., 1996) |
|---|---|---|---|---|
| IL-4 | 129 | 100[b] | 11.5/1.35/1.21 | 10.2/1.87/ 1.71 |
| IL-7 (Cosenza et al., 1997) | 153 | 21.4[b] | 0/0/0 | 13.9/2.08/1.95 |
| IL-7 (Kroemer et al., 1996) | 152 | 21.4[b] | 13.9/2.08/1.95 | 0/0/0 |

[a]Information represented as topological diversity score (TD)/RMS deviation/mean deviation between the C$\alpha$ atoms in matched residues.
[b]Represents the amino acid sequence similarity to IL-4.

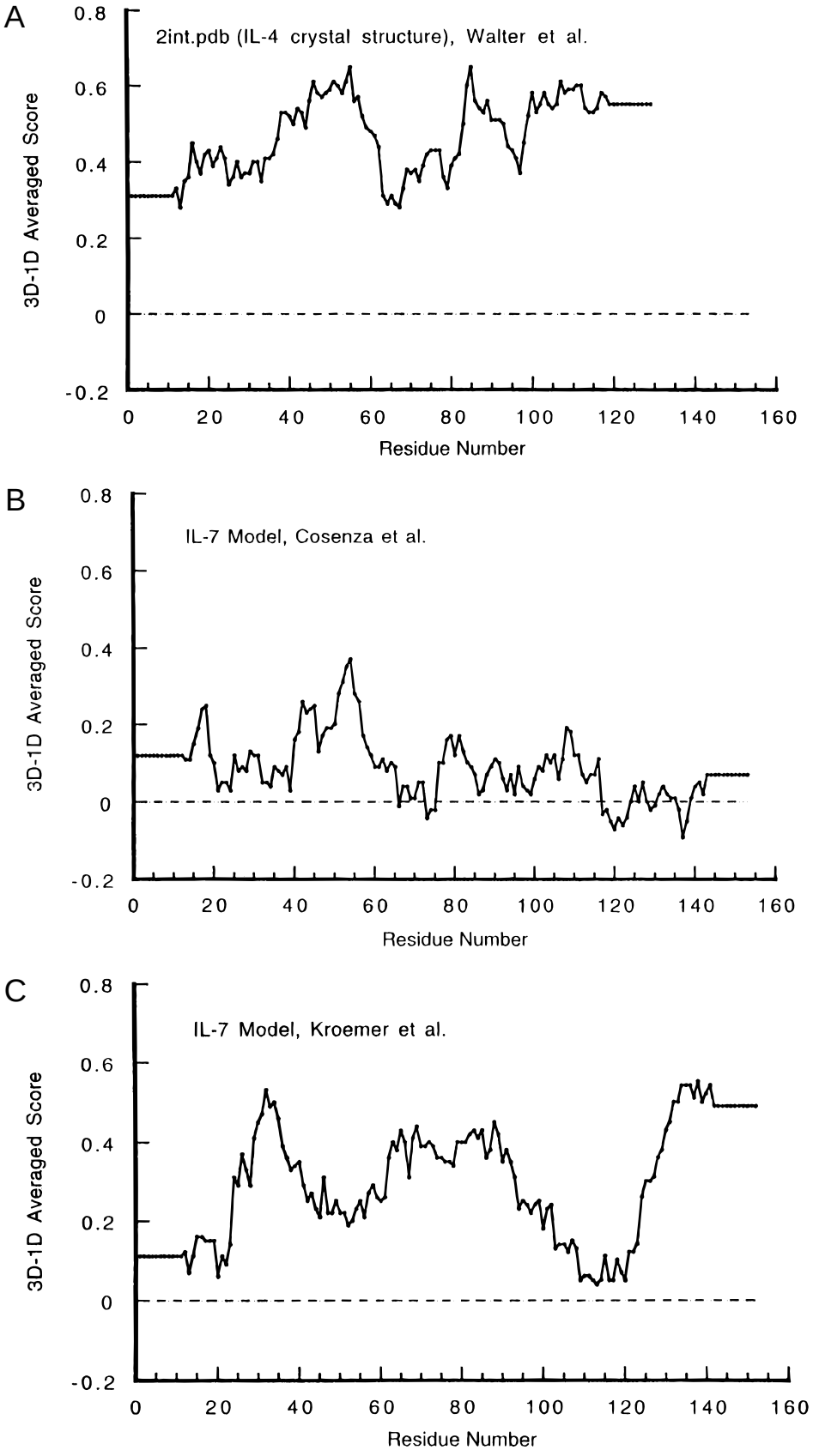


**Fig. 5.** Comparison of the 3D–1D profiles for the IL-4 template and IL-7 models. A comparison of the 21-window averaged profile score for IL-4 and the IL-7 models is plotted against residue position. **A:** IL-4 structure (2int.). **B:** Human IL-7 model generated in this work. **C:** Human IL-7 model generated by Kroemer et al. (1996).

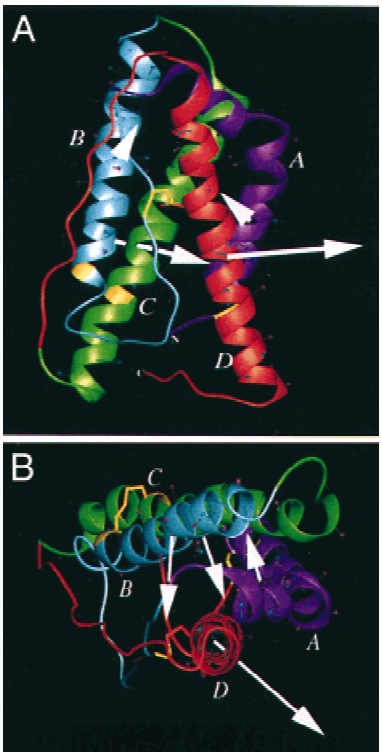


**Fig. 6.** A graphical representation of computed hydrophobic moments. **A:** Ribbon representation of the IL-7 model. The white vectors represent the net residue hydrophobic moments for each helix and have been placed at the center of each alpha helix. **B:** Same image rotated 90°. The helices are colored as in Figure 2.

The atypical surface chemistry as defined by the hydrophobic moment analysis of the IL-7 model may represent a region of amino acid sequence in the protein important for receptor binding and activation. Based upon the hydrophobic moment analysis of the IL-7 model, it is likely that the hIL-7 dimer formation seen in immunoblot analysis during protein expression and purification (Cosenza et al., 1997) may occur through interactions in predicted helix D. Because there is an apparent conservation of receptor binding surfaces localization on helices A and D of the alpha-parallel bundle cytokines, we anticipated that helix D of IL-7 may be important for receptor binding and activation. To test this hypothesis, nine amino acid residues corresponding to the solvent exposed surface of helix D were selected for site-directed Ala substitution scanning mutagenesis.

### *Site-directed Ala substitution scanning mutagenesis, construction, and characterization of IL-7 variants*

Based upon the predicted exposed surface of helix D in the IL-7 model, nine site-directed Ala substitutions were individually introduced into the hIL-7 DNA sequence using polymerase chain reaction mutagenesis. The mutated sequences were then digested with *Age*I and *Hin*dIII and vectorially subcloned into the synthetic hIL-7 structural gene by cassette replacement. Each mutant gene was then sequenced to ensure that only the desired Ala replacement mutation was incorporated. Native and hIL-7 Ala substitution mutants were expressed, purified, and their biologically activity measured.

The ability to stimulate 2E8 cell proliferation was compared for the native and hIL-7 Ala substitution mutants. Each of the hIL-7 variants K125A, N127A, D128A, L132A, and L147A was found to stimulate the growth of 2E8 cells with a dose response similar to wild-type IL-7 ($EC_{50}$ $3 \times 10^{-10}$ M each, data not shown). In contrast, the replacement of amino acid residues K121, L136, K140, and W143 with Ala resulted in hIL-7 variants with altered biologic activity when compared to native hIL-7 (Fig. 7). The mutant hIL-7 (K121A) displayed a biphasic response in the ability to stimulate 2E8 cell proliferation. The mutants hIL-7(L136A) and hIL-7 (K140A) were found to stimulate cell proliferation with $EC_{50}$ of $2.0 \times 10^{-9}$ M and $4 \times 10^{-9}$ M, respectively. In marked contrast, the mutant hIL-7(W143A) was found to be biologically inactive.

### *Competitive binding analysis*

To investigate if the biological effects resulting from Ala substitution mutations in hIL-7 were related to receptor affinity, competitive binding assays were performed using [$^{125}$I]-hIL-7. A constant amount of [$^{125}$I]-hIL-7 was incubated with $1 \times 10^6$ NALM-6 cells in the absence or presence of increasing concentrations of native or mutant hIL-7 for 30 min at 37 °C. Bound radioactivity was separated from free by centrifuging cells through NYSOL oil and counted. The amount of [$^{125}$I]-hIL-7 bound in the absence and presence of hIL-7 variants was measured and the concentration required to displace 50% of the bound radioactivity ($IC_{50}$) was determined. A summary of $IC_{50}$ and $EC_{50}$ values measured for native and hIL-7 Ala substitution mutants is displayed in Table 2. Native hIL-7 resulted in an $IC_{50}$ of $2.2 \times 10^{-9}$ M. Ala substitution

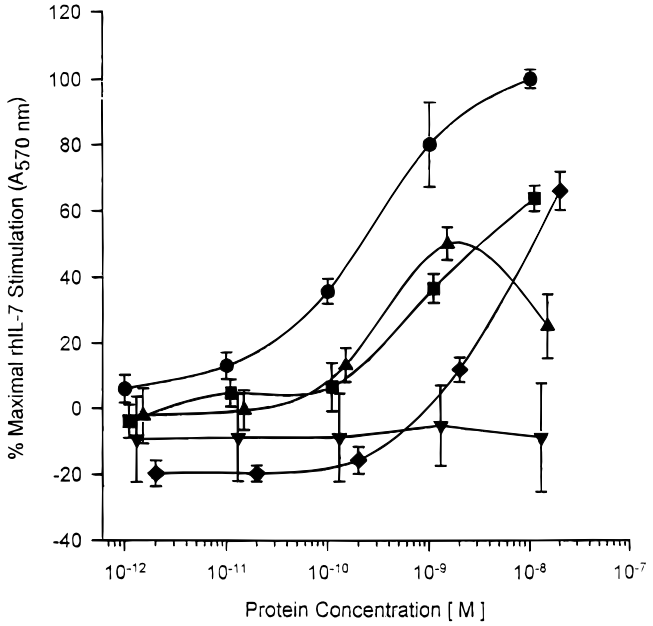


**Fig. 7.** Comparison of dose response analysis of Ala substitution hIL-7 variants. The ability of native and Ala substitution hIL-7 variants K121A, L136A, K140A, and W143A to stimulate 2E8 cell proliferation is compared. Cell proliferation in the presence of increasing protein concentrations was measured and the results as % maximal hIL-7 stimulation ($A_{570nm}$). The concentration of hIL-7 that gives maximal stimulation in our assay is $1 \times 10^{-8}$ M was used to computer percentages ($n = 4$). ●, RhIL-7; ▲, rhIL-7(K121A); ♦, rhIL-7(L136A); ■, rhIL-7(K140A); ▼, rhIL-7(W143A).

**Table 2.** *Summary of $IC_{50}$ and $EC_{50}$ values for hIL-7 and hIL-7 variants*

| Protein | $IC_{50}$ (M)[a] | $EC_{50}$ (M)[a] | $EC_{50}/EC_{50}$ (variant/hIL-7) |
|---|---|---|---|
| hIL-7 | $2.2 \times 10^{-9}$ | $3.0 \times 10^{-10}$ | 1.0 |
| hIL-7(K121A) | $3.0 \times 10^{-8}$ | $7.0 \times 10^{-9}/4.0 \times 10^{-10}$ | 23/1.3 |
| hIL-7(K125A) | — | $3.0 \times 10^{-10}$ | 1.0 |
| hIL-7(N127A) | — | $3.0 \times 10^{-10}$ | 1.0 |
| hIL-7(D128A) | — | $3.0 \times 10^{-10}$ | 1.0 |
| hIL-7(L132A) | — | $3.0 \times 10^{-10}$ | 1.0 |
| hIL-7(L136A) | $5 \times 10^{-9}$ | $2.0 \times 10^{-9}$ | 6.7 |
| hIL-7(K140A) | $1 \times 10^{-8}$ | $4.0 \times 10^{-9}$ | 6.7 |
| hIL-7(W143A) | $2 \times 10^{-8}$ | $>1.6 \times 10^{-6}$ | 5,333.3 |
| hIL-7(L147A) | — | $3.0 \times 10^{-1}$ | 1.0 |

[a] Estimates only, $IC_{50}$ values derived from competitive binding assays on Nalm-6 cell line and $EC_{50}$ values derived from 2E8 cell proliferation assays.

mutants hIL-7(K121A), hIL-7(L136A), and hIL-7(K140A) displayed $IC_{50}$ values of $3.0 \times 10^{-9}$ M, $5.0 \times 10^{-9}$ M, and $1.0 \times 10^{-8}$ M, respectively. The biologically inactive mutant hIL-7 (W143A) displayed an $IC_{50}$ of $2.0 \times 10^{-8}$ M. A graphical summary of the Ala scanning mutagenesis in hIL-7 is displayed in Figure 8.

## Discussion

A factor that we believe played a major role in reducing the overall quality of the IL-7 model generated in this work was the calculated hydrophobic moment of helix D oriented toward bulk solvent. The overall quality of the IL-7 model generated in this work was poor when compared either to the template IL-4 structure or the IL-7 model generated by Kroemer et al. (1996). The model developed by Kroemer et al. is a four-alpha helical bundle created from RMS superimpositions of C$\alpha$ atoms from GH, IL-2, IL-4, and GM-CSF and constructed by homologous extension. It differs from ours in the disulfide bond assignments. The disulfide bond assignment that Kroemer et al. (1996) used was generated by Srinivasan et al. (1993). The reason for the discrepancy in the disulfide bond assignments is unknown; there is the possibility that there are other isoforms of human IL-7 with altered patterns of disulfide bonding. Two other isoforms of IL-7 were described during the cloning of IL-7 by Goodwin et al. (1989), which recently have been rediscovered in intestinal epithelial cells by Madrigal-Estebas et al. (1997), and apparently encode carboxyl terminal truncated proteins that failed to display biological activity. This naturally occurring helix D deletion mutant suggests that biological activity is associated with the carboxyl terminal of human IL-7. The disulfide bond assignments used in this work were generated from a combination of MALDI mass spectroscopy and site-directed mutagenesis analyses (Cosenza et al., 1997). Interestingly, these disulfide bond assignments forced the amino and carboxyl terminal of the protein into close proximity and reorientated helix D, exposing a hydrophobic patch of residues to bulk solvent. Because of the atypical orientation of helix D, we believed that either the model was incorrect or that helix D may play a role in protein–protein interactions important for IL-7 biological activity.

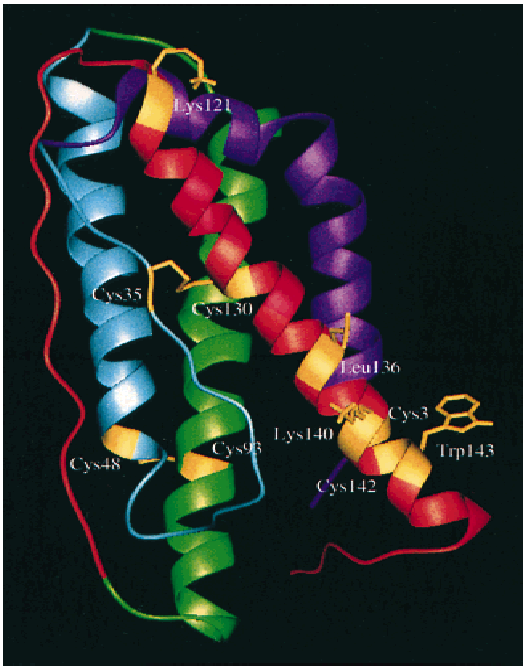


**Fig. 8.** Ala-substitution mutagenized positions. Helix D is displayed with amino acids residues selected for site-directed alanine substitution mutagenesis and are highlighted in yellow and red. The residues K121, L136, K140, and W143, which have been shown to be effected by IL-7 function (see Fig. 7), are displayed with a stick representation of their side chains.

The hydrophobic moment analysis of helix D in the IL-7 model highlighted a sequence of amino acid residues important for receptor binding and activation. Mutational studies in helical cytokines have defined three surface regions that can interact with receptor (Barton et al., 1999), although on any particular cytokine all three regions do not have to be involved in binding. Many of the mutations that help define regions of receptor interaction in the helical cytokines with known structures are located in helices A and D (Mott & Campbell, 1995). These phenomena have suggested that there is a conserved mechanism for receptor binding among the cytokines (Bazan, 1990a). In this case, the solvent exposed hydrophobic surface of the IL-7 model would energetically favor protein interactions for receptor binding and might explain dimer formation seen during expression and purification (Cosenza et al., 1997). This hypothesis was tested using site-directed Ala substitution-scanning mutagenesis along the carboxyl terminus of hIL-7. Site-directed Ala substitution-scanning mutagenesis of amino acids corresponding to helix D in the model resulted in constructing nine variants, of which four displayed reduced biologic activity and could displace [$^{125}$I]-hIL-7. Amino acid substitutions K121A, L136A, K140A, and W143A in human IL-7 resulted in mutants that reduced or abrogated the ability to stimulate 2E8 pre-B cell proliferation, in vitro. The substitution mutations L136A, K140A, and W143A form a patch near the carboxyl terminal of helix D in the IL-7 model. The variant located at the very amino terminal of helix D, hIL-7(K121A), displayed a biphasic proliferation curve that we believe is a result of reduced solubility at the higher protein concentrations. As anticipated, progression of the mutational analysis through a receptor-binding surface generated hIL-7 variants with reduced ability to stimulate 2E8 cell proliferation, in vitro. When the position of the site-directed substitution moved past the receptor binding surface, full biological activity was recovered as displayed by hIL-7(L147A).

Mutational analysis of the carboxyl terminus of a structurally related cytokine, IL-4, resulted in the construction and identification of a receptor antagonist. In an effort to distinguish amino acid residues in IL-4 responsible for binding or receptor activation, single substitutions at cysteine and aromatic residues were constructed. The aromatic residue, Tyr124, in IL-4 when mutated to aspartic acid, resulted in the production of a high-affinity antagonist to the IL-4 receptor (Kruse et al., 1992, 1993). This work eventually produced the high-affinity IL-4 receptor antagonist IL-4(Y124D). In the case of hIL-7, the lack of activity displayed by IL-7(W143A) suggested that Trp143 is important for receptor binding and activation and consequently aligns directly with the Y124 in IL-4, as shown in Figure 3A.

Recent literature diverges on the mechanisms for cytokine receptor binding and activation. It is understood that homo- or heterodimerization is necessary for the activation of signal transduction associated with the Type 1 cytokine receptor structural family. Early literature regarding cytokine receptor binding was characterized by ligands acting as molecular bridges facilitating or inducing dimerization and eventual activation. This mechanism was first supported by the mutagenesis and X-ray crystal structure analyses of human growth hormone bound to its receptor (deVos et al., 1992). More recently, this molecular bridge paradigm is supported by the structural determination of the IL-4/receptor $\alpha$ intermediate. Here, IL-4 binds to its receptor $\alpha$ protein and then using its carboxyl terminal helix D recruits the IL-2 common $\gamma$ chain, which then forms the high-affinity signal transducing complex with the ligand acting as a linker (Hage et al., 1999). Results from recent work support mechanisms that diverge from the molecular bridging paradigm and suggest that binding induces structural reorientations in preformed receptor complexes. For example, the use of fluorescence resonant energy transfer studies of the IL-2R, IL-7R, and IL-15R suggests that these proteins cluster on the surface of the cell membrane and that ligand binding stabilizes an active receptor complex (Damjanovich et al., 1997). The X-ray crystal structures of erythropoietin receptor in its bound and unbound states suggest that it exists as a preformed dimmer, and that ligand binding induces spatial reorientation that starts the signal transduction cascade (Livnah et al., 1999). Ultimately, the differences in the mechanistic models for receptor binding will be reflected in the strategies used for drug design.

We propose that the IL-7 variant IL-7(W143A) abrogates 2E8 cell proliferation by failing to activate JAK3, a kinase important for IL-7R signaling. The IL-4 and IL-7 receptors belong to the same structural family, and both cytokine binding complexes incorporate the IL-2 common $\gamma$-chain. The IL-2 common $\gamma$-chain can associate with Janus kinases (JAK), in particular JAK3 (Chen et al., 1997). Interestingly, constitutive activation of the IL-7R-JAK3-STAT signal pathways by v-Abl results in cancer (Banerjee & Rothman, 1998; Hilbert et al., 1998). The X-ray crystal structure of IL-4 bound to its receptor suggests that helix D recruits the IL-2R common $\gamma$-chain. The hIL-7 mutants L136A, K140A and W143A form a receptor binding patch near the carboxyl terminus of the protein that displayed altered the ability to induce 2E8 cell proliferation yet could bind receptor. Based upon the reported structural biology of IL-4/IL-4R and our helix D mutants, we believe that the residues located at the carboxyl terminal of helix D are important for positional recruitment and binding to the common IL-2R $\gamma$-chain and activation of JAK3.

In summary, the analysis of a tertiary structural hypothesis for human IL-7 led to structure–activity relationships that defined a receptor binding surface on the ligand and construction and characterization of IL-7(W143A), the first IL-7R antagonist. An IL-7 structural hypothesis was developed using a probabilistic sequence structure recognition analysis that determined the protein folding-class model and secondary structures. The construction of the IL-7 model proceeded by comparative model building using the structure of IL-4 as a template. The construction of the atomic scale 3D IL-7 structure was completed after inserting the experimentally assigned disulfide bonds and energetically minimizing the model. Analysis of the structure and previously published biochemical evidence led to the hypothesis that helix D was important for biological activity, which was tested using site-directed Ala substitution mutagenesis. A consequence of investigating IL-7 receptor binding by site-directed Ala scanning mutagenesis analysis is the construction of mutant hIL-7(W143A), which is biologically inactive and appears to bind to IL-7R and, thus, is the first reported antagonist of the IL-7 receptor system.

## Materials and methods

### *Amino acid sequence analysis*

The analysis is an extension of inverse folding methodology (Bowie & Eisenberg, 1993). Probabilistic models (DSMs) are constructed for sequences that are compatible with the secondary structural constraints implied by specific folding classes. The probability (likelihood) that any such DSM would generate the hIL-7 sequence is easily computed using an optimal filtering algorithm (White et al., 1994). From these model likelihoods, the probability of each model having generated the sequence is computed using Bayes's rule in probability theory. The prior probabilities of the models are selected to be uninformative, given the hierarchical structure of the DSM library. Once the most probable DSMs are identified, they are used, together with an optimal smoothing algorithm (Stultz et al., 1993), to estimate the secondary structural state of each residue in the sequence. An introduction to this probabilistic approach is presented in Stultz et al. (1997). An e-mail server that provides DSM-based sequence analysis is available on the World Wide Web (PSA e-mail server, http://bmerc-www.bu.edu/psa).

### *Construction of IL-7 protein model*

Virtual construction of the IL-7 model was performed using QUANTA software as a graphical interface to an Indigo 2 (Silicon Graphics Inc., Mountain View, California) to construct 3D structural models. Structural hypothesis of IL-7 was built by comparative modeling using the IL-4 X-ray crystal structure as a template for alpha-parallel bundles. Secondary structure assignments from the amino acid sequence analysis of IL-7 were used to model helices that formed the core of our models. Core helices were superimposed upon the template, and their hydrophobic moments (Eisenberg et al., 1982) evaluated so as to ensure maximal packing of hydrophobic residues in the interior of the model. The remaining IL-7 amino acid sequences were used as loops that connected helices and were modeled using a bond scaling and relaxation algorithm (Zheng et al., 1992). Disulfide bonds were assigned, and the resultant structure was energetically minimized. Energy minimizations were performed using the program CHARMM (Brooks et al., 1983) using an empirical energy function that included con-

formational energy terms, van der Waals forces, and electrostatic potentials. A steepest descent method for 500 cycles was used to reduce steric hindrances and dihedral angle strain.

### *Expression and purification of IL-7*

Recombinant hIL-7 and hIL-7 variant protein were expressed, purified, and refolded from *Escherichia coli* HMS174(DE3)pLysS as previously reported (Cosenza et al., 1997). Briefly, native and mutant IL-7 proteins were expressed under the control of a T7 RNA polymerase promoter in derivatives of pET11d. Recombinant protein expression was induced by the addition IPTG. Following a 2-h incubation, bacteria were harvested by centrifugation ($5{,}000 \times g$), and the pellet was frozen at $-20\,^{\circ}$C. Frozen bacterial pellets were thawed and resuspended in lysis buffer. The bacteria were lysed by pulsed sonication. In this expression system, overexpressed hIL-7 protein forms insoluble inclusion bodies. The inclusion bodies were purified by centrifugation, washed three times, and then resuspended in denaturation buffer (50 mM Tris-HCl, pH 8, 5 M guanidine hydrochloride, 5 mM EDTA), and sonicated briefly. Dithiothreitol (DTT) was added to a final concentration of 6 mM. Denatured IL-7 proteins were further purified by guanidine HPLC sizing. Protein preparations were refolded to a biologically active conformation and further purified by native HPLC sizing. Protein concentrations were determined by the Bradford method (Pierce Chemical Co., Rockford, Illinois) and then stored at $-70\,^{\circ}$C until used.

### *CD analysis*

An absorption spectrum was recorded using a Model 62DS Circular Spectrometer (AVIV, Lakewood, New Jersey). Samples were pre-filtered with a 0.22-$\mu$m Millipore filter, and spectra were obtained using a 1-cm pathlength cell with a protein concentration of 0.2 mg/mL in 10 mM phosphate buffer, pH 7.0. The spectrum is the average of three scans ranging from 190–250 nm. A solvent spectrum was subtracted from each protein sample. The reported spectrum is expressed as molar ellipticity and calculated by using a mean residue weight of 115.

### *IL-7 biological assay*

Recombinant hIL-7 and related mutant proteins were tested for their ability to induce the proliferation of the IL-7–dependent murine immature B lymphocyte cell line 2E8 (ATCC TIB 239) in vitro. 2E8 cells were maintained in Isocove's modified Dulbecco's medium (Gibco, Grand Island, New York) supplemented with 0.05 mM 2-mercaptoethanol (2-ME), 2 mM glutamine, 50 IU/mL penicillin, 50 $\mu$g/mL streptomycin, 5 ng/mL IL-7, and 5% fetal calf serum (Cellect, Gibco), at 37 °C in a 5% $CO_2$ atmosphere. IL-7 remains biologically active in the presence of 0.05 mM 2-ME. Cell proliferation was measured by MTT [3-(4,5-dimethylthazol-2-yl)-2,5-diphenyl tetrazolium bromide salt] absorbance at 570 nm following reduction by active mitochondria. For proliferation assays, 2E8 cells were washed three times, and seeded in 96-well plates (Linbro, Flow Laboratories, McLean, Virginia) in 50 $\mu$L of IL-7 free media at a density of $1 \times 10^5$ cells/well. Fifty microliter aliquots of protein were added to each well to give a range of concentrations from $10^{-12}$ to $10^{-8}$ M in a final volume of 100 $\mu$L. After a 48-h incubation, 30 $\mu$L MTT (5 mg/mL) were added to each well and incubated at 37 °C for 2 h. The formazan crystals were then solubilized by adding 100 $\mu$L of 20% SDS in 50% DMF (dimethyl formamide, pH 4.7) and incubating at 37 °C overnight (Hansen et al., 1989). The following day the absorbance of the formazan product was measured on an ELISA plate reader at 570 nm.

### *Competitive displacement assays*

Iodination of biologically active hIL-7 was performed in a hood according to safety guidelines issued by the Boston University Radiation Safety Office and OSHA using IODO-BEADS (Pierce). Briefly, aliquots of 300 $\mu$g of hIL-7 were iodinated using carrier free $Na^{125}I$ (DuPont NEN, Boston, Massachusetts) in a working volume of 500 $\mu$L of PBS for 15 min at room temperature. The reaction was terminated by removal of the IODO beads and radiolabeled protein was purified from unincorporated $^{125}I$ by G25 Sephadex sizing column with complete media as the mobile phase.

The displacement of [$^{125}$I]-hIL-7 from IL-7 receptors bearing cells was performed essentially according to the procedure described by Wang and Smith (1987). Nalm-6 cells were harvested, washed three times with culture medium and resuspended to $1 \times 10^7$ per mL. Microcentrifuge tubes were prepared by adding 100 $\mu$L NYSOL, a constant concentration of [$^{125}$I]-hIL-7 in the absence or presence of increasing concentrations of unlabeled native or mutant hIL-7 to a final volume of 100 $\mu$L. The displacement reactions were started by the addition of 100 $\mu$L of cells to each tube. The reaction mixtures were incubated for 30 min at 37 °C, and then the cells were centrifuged through the NYSOL oil. The cell pellets and supernatants, representing bound and free radioactivity, respectively, were separated by clipping the tips of the tubes. The radioactivity in the pellets and supernatants were counted in a Beckman Gamma 5500 counter. The concentrations of unlabeled ligand required to displace 50% of [$^{125}$I]-hIL-7 binding ($IC_{50}$) from the IL-7 receptor bearing Nalm-6 cells was measured.

## Acknowledgments

These studies were supported by grants (U19 CA48626-08 and P41 RR10888-02) from the National Institutes of Health. We would like to Drs. Toby Hecht and Mary Wolpert for all of their administrative support, and Dr. Steven Giardina, located at the Monoclonal Antibody and Recombinant Protein Facility, for his role as part of the NCDDG contract, and supplying research grade interleukin-7. The PSA (Protein Sequence Analysis) e-mail server, maintained by Boston University and TASC, Inc., has the URL http://bmerc-www.bu.edu/psa and the e-mail address psa-request@darwin.bu.edu. For information, send an empty message with the word "help" in the subject field.

## References

Alderson MR, Sassenfeld HM, Widmer MB. 1991. Interleukin 7 induces cytokine secretion and tumoricidal activity by human peripheral blood monocytes. *J Exp Med 173*:923–930.

Bajorath J, Stenkamp R, Aruffo A. 1993. Knowledge-based model building of proteins: Concepts and examples. *Protein Sci 2*:1798–1810.

Banerjee A, Rothman P. 1998. Il-7 reconstitutes multiple aspects of v-Abl-Mediated signaling. *J Immunol 161*:4611–4617.

Barton VA, Hudson KR, Heath JK. 1999. Identification of three distinct receptor binding sites of murine interleukin-II. *J Biol Chem 274*:5755–5761.

Bazan JF. 1990a. Haemopoietic receptors and helical cytokines. *Immunol Today 11*:350–354.

Bazan JF. 1990b. Structural design and molecular evolution of a cytokine receptor superfamily. *Proc Natl Acad Sci USA 87*:6934–6938.

Bernstein FC, Koetzle TF, Williams GJ, Meyer EE Jr, Brice MD, Rodgers JR, Kennard O, Shimanouchi T, Tasumi M. 1977. The Protein Data Bank: A

computer-based archival file for macromolecular structures. *J Mol Biol 112*:535–542.
Bowie JU, Eisenberg D. 1993. Inverted protein structure prediction. *Curr Opin Struct Biol 3*:437–444.
Brooks BR, Bruccoleri RE, Olafson BD, States DJ, Swaminathan S, Karplus M. 1983. CHARMM: A program for macromolecular energy, minimization, and dynamics calculations. *J Comput Chem 4*:187–217.
Chazen GD, Pereira GMB, LeGros G, Gillis S, Shevach EM. 1989. Interleukin 7 is a T-cell growth factor. *Proc Natl Acad Sci USA 86*:5923–5927.
Chen M, Cheng A, Chen YQ, Hymel A, Hanson EP, Kimmel L, Minami Y, Taniguchi T, Changelian PS, O'Shea JJ. 1997. The amino terminus of JAK3 is necessary and sufficient for binding to the common gamma chain and confers the ability to transmit interleukin 2-mediated signals. *Proc Natl Acad Sci USA 94*:6910–6915.
Chou PY, Fasman GD. 1978. Prediction of the secondary structure of proteins from their amino acid sequence. *Adv Enzymol 47*:45–148.
Cosenza L, Sweeney E, Murphy JR. 1997. Disulfide bond assignment in human interleukin-7 by matrix-assisted lase desorption/ionization mass spectroscopy and site-directed cysteine to serine mutational analysis. *J Biol Chem 272*:32995–33000.
Damjanovich S, Bene L, Matko J, Alileche A, Goldman CK, Sharrow S, Waldmann TA. 1997. Preassembly of interleukin 2 (IL2) receptor subunits on resting Kit 225 K6 T cells and their modulation by IL-2, IL-7, and IL-15: A fluorescence resonance energy transfer study. *Proc Natl Acad Sci USA 94*:13134–13139.
deVos AM, Ultsch M, Kossiakoff AA. 1992. Human growth hormone and extracellular domain of its receptor: Crystal structure of the complex. *Science 255*:306–312.
Di Santo JP, Kuhn R, Muller W. 1995. Common cytokine receptor gamma chain (gamma c)-dependent cytokines: Understanding in vivo functions by gene targeting. *Immunol Rev 148*:19–34.
Eisenberg D, Weiss RM, Terwilliger TC, Wilcox W. 1982. Hydrophobic moments and protein structure. *Faraday Symp Chem Soc 17*:109–120.
Fasman GD. 1989. *Prediction of protein structure and the principles of protein conformation*. New York: Plenum Press.
Garnier J, Osguthorpe DJ, Robson B. 1978. Analysis of the accuracy and implications of simple methods for predicting the secondary structure of globular proteins. *J Mol Biol 120*:97–120.
Goodwin RG, Lupton S, Schmierer A, Hjerrild KJ, Jerzy R, Clevenger W, Gillis S, Cosman D, Namen AE. 1989. Human interleukin-7: Molecular cloning and growth factor activity on human and murine B-lineage cells. *Proc Natl Acad Sci USA 86*:302–306.
Hage T, Sebald W, Reinemer P. 1999. Crystal structure of the interleukin-4/receptor alpha chain complex reveals a mosaic binding interface. *Cell 97*:271–281.
Hansen M, Nielson S, Berg K. 1989. Re-examination and further development of a precise and rapid dye method for measuring cell growth/cell kill. *J Immunol Methods 119*:203–210.
Hilbert DM, Theisen PW, Rudikoff EK, Bauer SR. 1998. Interaction of abl and raf with IL-7 signaling pathway and transformation of pre-B cells from resistant mice. *Oncogene 17*:2125–2135.
Kroemer RT, Doughty SW, Robinson AJ, Richards WG. 1996. Prediction of the three-dimensional structure of human interleukin-7 by homology modeling. *Protein Eng 9*:493–498.
Kruse N, Shen B-J, Arnold S, Tony H-P, Muller T, Sebald W. 1993. Two distinct functional sites of human interleukin 4 are identified by variants impared in either receptor binding or receptor activation. *EMBO J 12*:5121–5129.
Kruse N, Tony H-P, Sebald W. 1992. Conversion of human interleukin-4 into a high affinity antagonist by a single amino acid replacement. *EMBO J 11*:3237–3244.
Livnah O, Stura EA, Middleton SA, Johnson DL, Jolliffe LK, Wilson IA. 1999. Crystallographic evidence for preformed dimers of erythropoietin receptor before ligand activation. *Science 283*:987–990.
Londei M, Verhoef A, Hawrylowicz C, Groves J, De Berardinis P, Feldmann M. 1990. Interleukin-7 is a growth factor for mature human T cells. *Eur J Immunol 20*:425–428.
Lu G. 1996. A WWW service for automated comparison of protein structures. *Protein Data Bank Q Newslett 78*:10–11.
Lu G. 1998. An approach for multiple alignment of protein structures. *Struct Fold Des*. Forthcoming. http://gamma.mbb.ki.se/~guoguang.
Luthy R, Bowie JU, Eisenberg D. 1992. Assessment of protein models with three-dimensional profiles. *Nature 356*:83–85.
Madrigal-Estebas L, McManus R, Byrne B, Lynch S, Doherty DG, Kelleher D, O'Donoghue DP, Feighery C, O'Farrelly C. 1997. Human small intestinal epithelial cells secrete interleukin-7 and differentially express two different interleukin-7 mRNA transcripts: Implications for extrathymic T-cell differentiation. *Hum Immunol 58*:83–90.
Maeurer MJ, Lotze MT. 1998. Interleukin-7 (IL-7) knockout mice. Implications for lymphopoiesis and organ-specific immunity. *Int Rev Immunol 16*:309–322.
Maki K, Sunaga S, Ikuta K. 1998. The V-J recombination of T cell receptor-gamma genes is blocked in interleukin-7 receptor-deficient mice. *Int Rev Immunol 16*:285–308.
Mertsching E, Meyer V, Linares J, Lombard-Platet S, Ceredig R. 1997. Interleukin-7, a non-redundant potent cytokine whose over-expression massively perturbs B-lymphopoiesis. *J Immunol 159*:3044–3056.
Mott HR, Campbell ID. 1995. Four-helix bundle growth factors and their receptors: Protein–protein interactions. *Curr Opin Struct Biol 5*:114–121.
Murphy WJ, Back TC, Conlon KC, Komschlies KL, Ortaldo JR, Sayers TJ, Wiltrout RH, Longo DL. 1993. Antitumor effects of interleukin-7 and adoptive immunotherapy on human colon carcinoma xenografts. *J Clin Invest 92*:1918–1924.
Namen AE, Lupton S, Hjerrild K, Wignall J, Mochizuki DY, Schmierer A, Mosley B, March CJ, Urdal D, Gillis S, et al. 1988. Stimulation of B-cell progenitors by cloned murine interleukin-7. *Nature 333*:571–573.
Parry DAD. 1991. Cytokine conformations: Predictive studies. *J Mol Recognit 4*:63–75.
Sprang SR, Bazan JF. 1993. Cytokine structural taxonomy and mechanisms of receptor engagement. *Curr Opin Struct Biol 3*:815–827.
Srinivasan S, Deeley MC, Park LS, March CJ, Sassenfeld H, Sudarsanam S. 1993. A model of IL-7 and extra-cellular domains of its receptor complex using distance geometry and structure–function data. *Protein Eng (Suppl) 6*:107.
Stultz CM, Nambudripad R, Lathrop RH, White JV. 1997. Predicting protein structure with probabilistic models. In: Allewell N, Woodward C, eds. *Protein structural biology in bio-medical research*, vol. B. Greenwich: JAI Press.
Stultz CM, White JV, Smith TF. 1993. Structural analysis based on state-space modeling. *Protein Sci 2*:305–314.
Walter MR, Cook WJ, Ealick SE, Nagabhushan TL, Trotta PP, Bugg CE. 1992a. Three-dimensional structure of recombinant human granulocyte-macrophage colony-stimulating factor. *J Mol Biol 224*:1075–1085.
Walter MR, Cook WJ, Zhao BG, Cameron RP Jr, Ealick SE, Walter RL Jr, Reichert P, Nagabhushan TL, Trotta PP, Bugg CE. 1992b. Crystal structure of recombinant human interleukin-4. *J Biol Chem 267*:20371–20376.
Wang H-M, Smith KA. 1987. The interleukin 2 receptor. *J Exp Med 166*:1055–1069.
Watanabe M, Ueno Y, Yajima T, Okamoto S, Hayashi T, Yamazaki M, Iwao Y, Ishii H, Habu S, Uehira M, et al. 1998. Interleukin 7 transgenic mice develop chronic colitis with decreased interleukin 7 protein accumulation in the colonic mucosa. *J Exp Med 187*:389–402.
Welch PA, Namen AE, Goodwin RG, Armitage R, Cooper MD. 1989. Human IL-7: A novel T cell growth factor. *J Immunol 143*:3562–3567.
White JV, Stultz CM, Smith TF. 1994. Protein classification by stochastic modeling and optimal filtering of amino-acid sequences. *Math Biosci 119*: 35–75.
Wlodawer A, Pavlovsky A, Gustchina A. 1993. Hematopoietic cytokines: Similarities and differences in the structure, with implications for receptor binding. *Protein Sci 2*:1373–1382.
Yu L, White JV, Smith TF. 1998. A homology identification method that combines protein sequence and structure information. *Protein Sci 7*:2499–2510.
Zheng Q, Rosenfeld R, Vajda S, DeLisi C. 1992. Loop closure via bond scaling and relaxation. *J Comput Chem 14*:556–565.